PFS-REM: Robust Low-Complexity Classification of LOS/NLOS/Multipath in UWB Indoor Positioning

Original Scientific Paper

Gita Indah Hapsari*
Telkom University, School of Computing,
Department of Doctoral Informatics
Telekomunikasi Street, Bandung, Indonesia
gitaindahhapsari@telkomuniversity.ac.id

Bayu Erfianto
Telkom University, School of Computing,
Department of Doctoral Informatics
Telekomunikasi Street, Bandung, Indonesia
erfianto@telkomuniversity.ac.id

Rendy Munadi
Telkom University, School of Electrical Engineering,
Department of Telecommunication Engineering
Telekomunikasi Street, Bandung, Indonesia
rendymunadi@telkomuniversity.ac.id

Indrarini Dyah Irawati
Telkom University, School of Applied Science,
Department of Telecommunication Technology
Telekomunikasi Street, Bandung, Indonesia
indrarini@telkomuniversity.ac.id

*Corresponding author

Abstract *– Ultra-wideband (UWB) signals face challenges owing to complex obstacles in non-line-of-sight (NLOS) and multipath propagation. Distinguishing between NLOS and multipath signal propagations is crucial for differentiating the positioning error corrections. The application of edge and real-time computing presents a challenge in producing a model that is both simple and highly accurate. This study presents PFS-REM, a compact multi-class dataset designed to classify LOS, NLOS, and multipath conditions while reducing model complexity. The dataset was developed using PFS to select five key features: RXPower, FPPower, CIR, SNR, and Ranging from a secondary dataset, followed by REM to minimize ranging errors by 93.3% using an ESP32 UWB Pro module with a DW1000 chip. Measurements were conducted in controlled environments with varied antenna orientations (direct, perpendicular, and opposite) to simulate real-world conditions. The experimental results show that classification models, notably RF (with 99.7% accuracy), trained on PFS-REM achieve an over 50% reduction in execution time compared to models using 12 features, while maintaining high performance. Feature analysis revealed distinct signal characteristics across line-of-sight (LOS), non-line-of-sight (NLOS), and multipath scenarios, enhancing the dataset reliability. This approach supports the development of lightweight models suitable for edge computing and real-time indoor positioning applications, addressing the trade-off between accuracy and computational efficiency in complex environments.*

Keywords*: Compact Multi-class Dataset, Feature Selection, Regression, Classification Model, UWB Indoor Positioning*

Received: October 22, 2025; Received in revised form: November 28, 2025; Accepted: November 28, 2025

1. INTRODUCTION

Indoor tag positioning estimates where tags are located on items such as smartphones, wearables (e.g., watches), robots, drones, and other assets. A tag emits a signal or message that is detected by an anchor; using geometric methods, the system infers the distance between the tag and anchor. An anchor is a device with known coordinates or a location-sensing module that helps compute the approximate position of the tag. Indoor positioning is widely used in systems that rely on location data for process control or monitoring, such as indoor tracking [1], navigation [2, 3], and intelligent transportation systems [4].

According to ITU-R SM.1757-0 [5], Ultra-Wideband (UWB) is a radio signal with a very large bandwidth, from 3.1 to 10.6 GHz, and a power level below 41.3 dBm/MHz. Its broad bandwidth also provides UWB resistance to narrowband interference [6]. Previous work [7] reports indoor positioning accuracy on the order of meters to centimeters and has a good trend in indoor positioning research [8]. Furthermore, the incorporation of ultra-wideband (UWB) technology into consumer devices, exemplified by Apple U1, Samsung SmartTag+, and automotive digital keys, alongside the IEEE 802.15.4z standard, has significantly expedited their commercial implementation. Although UWB generally outperforms other signals in terms of accuracy [9], its performance degrades as indoor obstacles become more complex [10]. Consequently, the key challenge for UWB-based indoor positioning is environmental complexity.

Obstacles create conditions such as NLOS and multipath, as shown in Fig. 1. NLOS can cause refraction and corresponding signal attenuation, whereas multipath (MP) leads to fading and reflections, such that the signal does not travel directly from the transmitter to the receiver. To address these effects, various recent studies have applied machine learning, which is a technological solution for addressing the complexity of obstacles in indoor positioning [11, 12]. Various machine learning models, such as support vector machines (SVMs) [13, 14], have been used to improve accuracy in complex indoor environments. Convolutional Neural Network (CNN) [15, 16], and Random Forest (RF) [17].

Over the past decade, a large body of work has attempted to identify and mitigate NLOS/multipath errors using channel impulse response (CIR) features, machine learning (ML), or deep neural networks (DNNs). The signal characteristics of the CIR are exploited to distinguish LOS, NLOS, and multipath with an RSSI-based approach [18], TDoA [19], TWR [17], and distance estimated from Time-of-Flight (ToF) [20]. It is very important to distinguish between NLOS and Multipath cases because the correction errors are different for positioning estimation in UWB indoor positioning [21].

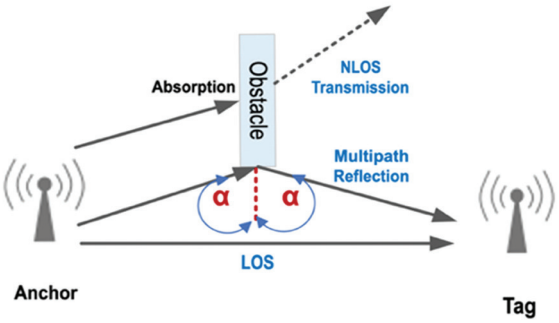

Fig. 1. LOS, NLOS, and Multipath signal propagation

However, only a few researchers have explicitly differentiated between NLOS and multipath signal propagation, which can potentially lead to larger positioning errors. Several studies have explicitly distinguished multipath propagation from NLOS presented in papers [22, 17]. Challenges remain in these studies on multipath, namely, the high complexity of the research [22], and the low accuracy in worst-case situations reported in [17].

In many practical implementations, datasets and models with low complexity are required because of the limited hardware, memory, and computational power of the target devices. Lightweight models facilitate the deployment of indoor positioning systems in edge computing environments or real-time positioning applications. Despite significant progress, these methods still suffer from high computational complexity, poor generalization across environments and hardware, and the inability to reliably distinguish pure NLOS from multipath-dominant conditions.

To date, no low-complexity, training-free method has demonstrated robust three-class (LOS/NLOS/multipath) identification capable of real-time execution on resource-constrained UWB devices while maintaining high accuracy across diverse environments and hardware platforms. To overcome these limitations, this paper introduces PFS-REM, a novel framework for robust, low-complexity classification of LOS, NLOS, and multipath UWB signal propagation conditions. The aim of this paper are i) create a dataset that can be used to identify LOS, NLOS and Multipath propagation signals, that has low complexity but high accuracy, ii) analyze each feature to observe the differences in signal characteristics of each LOS, NLOS and Multipath, and iii) produce a classification model of LOS, NLOS and Multipath that has low complexity and high accuracy. The contributions of this study are as follows:

- A compact Multi-class Dataset with selected features and error mitigation in LOS, NLOS, and multipath environments, so that it has high accuracy and lower complexity.
- A detailed feature analysis revealing distinct signal characteristics across propagation conditions, enhancing dataset reliability.
- An optimum model characterized by high accuracy and low complexity, capable of reliably identifying LOS, NLOS, and multipath signal propagation conditions.

2. RELATED WORK

In the past five years, ultra-wideband (UWB) channel classification has witnessed tremendous progress. This includes moving from simple line-of-sight (LOS) and non-line-of-sight (NLOS) classifications to more complex multi-class systems and from using manually created features to deep learning methods as shown in Table 1.

Early studies focused on lightweight binary classification using minimal features. Barral et al [23]. demonstrated that only two ranging statistics (mean and standard deviation of distance and RSSI) combined with Gaussian Process classification were sufficient to achieve 98.9 % accuracy on low-cost Pozyx devices that do not provide real-time Channel Impulse Response (CIR). Sang et al [17] extended the problem to three classes (LOS, NLOS, and explicit Multipath) using 12 CIR-derived statistical features and Random Forest, reporting 91.9 % accuracy while highlighting the distinct ranging bias introduced by the Multipath condition.

To improve robustness against distance- and power-dependent feature variations, Liu et al. [24] proposed the Practical NLOS Identification (PNI) framework with a reduce-effect-of-related-factors (REORF) normalization and five carefully selected CIR features, achieving 99.2 % accuracy in controlled laboratory settings and over 98 % in real-world environments using SVM. Hongchao Yang et al [13] introduced three novel CIR-derived parameters and a two-step Fuzzy Credibility-based SVM (FC-SVM), obtaining 93.3 % average accuracy across diverse scenarios and reducing final 2D positioning error to 9.1 cm after ranging mitigation.

Table 1. Dataset characteristic of recent paper

Author and Year	Year	Best Classifier	Class	Features/Selection	Accuracy
Barral et al. [23]	2019	Gaussian Process	2 class, LOS and NLOS	2 (Range and RSS)	98.9%
Sang et al. [17]	2020	RF	3 class LOS, NLOS, Multipath	12 CIR Stats	91.9%
Meiyu Liu et al. [24]	2021	SVM	2 class, LOS and NLOS	5+Normalisasi REORF	99.2%
Hongchao et al. [13]	2023	FC-SVM 2 Step	2 class, LOS and NLOS	9 Features CIR	93.3
Wang et al. [25]	2024	1D-CNN+LSTM+SE Attention	6 class, LOS and NLOS	Raw CIR 1016 Samples	95.6
Wang et al. [26]	2025	SVM+AREKF	2 class, LOS and NLOS	17 to 6-7 best Feature	97.6%
Wang et al. [27]	2025	FCE+XGBoost	2 class, LOS and NLOS	11 to 7-8best feature	93.2%
Majeed et al. [22]	2025	XGBoost+GA Tuning	6 class, Hard NLOS, Soft NLOS, Multipath	18 CIR Stats	99.47%
Proposed dataset	2025	CIR PFS-REM	3 LOS, NLOS, and Multipath	5 CIR Stats	99.7%

Recent studies have shifted toward multi-class classification using deep learning. Wang et al. [25] proposed 1D-CLANet, a lightweight 1D-CNN-LSTM network with Squeeze-and-Excitation attention operating directly on raw 1016-sample CIR waveforms, achieving 95.6 % accuracy in distinguishing four classes (LOS, NLOS-Wall, NLOS-Wood, NLOS-Human). Majeed et al. [22] reached the highest reported accuracy of 99.47 % using XGBoost with 18 hand-crafted features and genetic-algorithm-based tuning across five classes (LOS + four different NLOS materials/obstacles) on both public and local datasets.

Several authors have specifically addressed the mitigation of ranging errors and generalization. Wang and Ahmad [26] combined SVM-RFE feature selection with an Adaptive Robust Extended Kalman Filter (AREKF), reducing the 95th-percentile ranging error by 70–7Page 35 % compared to deep learning baselines. The same authors later [27] proposed a hybrid Fuzzy Comprehensive Evaluation (FCE) + XGBoost pipeline that, when trained in a single environment, maintained 93.2 % average accuracy across seven markedly different scenarios, demonstrating excellent cross-environment generalization.

Despite these advances, three critical limitations remain unresolved in the current literature.

- High-complexity methods (deep learning [25] or heavily tuned ensembles [22]) achieve excellent multi-class performance but are impractical for deployment on resource-constrained UWB anchors and tags.
- Works that explicitly separate the multipath condition [17][25] either sacrifice accuracy or rely on raw CIR processing, while lightweight approaches typically collapse Multipath into the NLOS class, losing the opportunity for class-specific error modeling.
- No existing solution simultaneously offers (i) robust three-class (LOS/NLOS/multipath) identification, (ii) an extremely small feature set suitable for real-time computation on low-end MCUs, (iii) high accuracy (>94 %) across highly diverse environments without retraining, and (iv) direct integration of a simple, class-specific Ranging Error Mitigation (REM) model.

The proposed PFS-REM framework directly addresses these gaps by introducing a Pareto-optimal feature selection stage, followed by a low-complexity classifier and class-aware error mitigation module, achieving state-of-the-art performance under strict computational and memory constraints typical of practical UWB indoor positioning systems.

3. MATERIAL AND METHOD

As illustrated in Fig. 2, the dataset construction process involves multiple systematic stages, including the selection of features from secondary datasets (Pearson feature selection (PFS)) and the mitigation of range errors (regression ranging error mitigation (REM)). These processes are fundamental for developing a proposed optimized dataset for accurate and efficient classification models. The explanation is accompanied by the stages of the research process algorithm in Table 2 for better understanding. The explanation sequence is based on the subsections presented in this section.

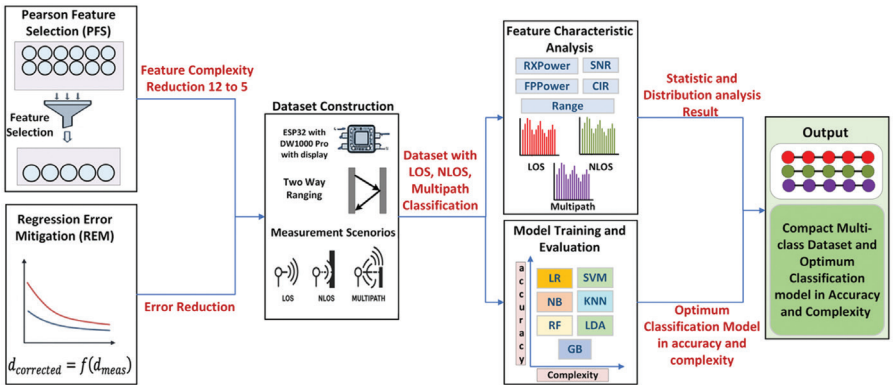

Fig. 2. Research Method

Table 2. Compact Multi-Class Dataset Construction for UWB Positioning Algorithm

Algorithm: Compact Multi-Class Dataset and Optimum classification model for UWB Positioning

1. Perform Feature Selection using Pearson Correlation (PFS)
   - Define feature set: $F=\{f_1, f_2, \ldots, f_{12}\}$, F is featuring set and f_n feature set before PFS.
   - Compute Pearson Correlation of each feature to target variable (equation 3)
   - Select reduce feature set (5 features): $F'=\{f'_1, f'_2, \ldots, f'_5\}$ where F' is feature set after PFS and fn' are the selected feature after PFS
2. Perform Regression Error Mitigation
   - Given Measure Distance: (d_{meas}) and Analyze error Ranging error (equation 4 and 5)
   - Apply Regression error correction model: $d_{corrected} = \beta_0 + \beta_1 . d_{meas} + \beta_2 . d_{meas}^2$
3. Construct Dataset from Measurement scenario
   - Define measurement scenario: LOS, NLOS, Multipath
   - For each scenario, measure ranging values using TWR: $r_n = c.t_{tof}$
   - Log feature set and corrected ranging Dataset Entry: $\{F', d_{corrected}, Label\}$
4. Perform Feature Characteristic Analysis
   - Analyze statistical distribution of features: RXPower, FPPower, SNR, CIR, Range
   - Compute correlation matrix among features
5. Train and Evaluate Multi-Class Classifier
   - Define Classifier: {LR, NB, GB, SVM, KNN, LDA} for each classifier compute: Accuracy and Complexity
   - Compute Performance: Select optimum model with highest accuracy, lowest complexity
6. Produce final compact multi-class dataset and optimum classification model
   - Output dataset: feature dimension, corrected ranging, multiclass labelling
   - Output optimum model classification: RF, KNN, GB

3.1. PEARSON FEATURE SELECTION (PFS)

PFS is based on a feature selection process [28] from a previous study to identify and select the most effective features. The objective of feature selection is to reduce computational complexity, enhance interpretability, and prevent information redundancy and overfitting in model development. Pearson's correlation was used to assess the correlation between features, selecting the features with the highest correlation in the hope of maintaining high classification model accuracy despite the reduced number of features.

Feature selection is method to reduce model complexity in machine learning [12, 29, 30]. PFS was conducted using a secondary dataset from Sang's research [17, 31], which originally comprised 12 features $F=\{f_1, f_2, \ldots, f_{12}\}$. The initial step in feature selection involved removing features that were directly related to other calculated features. The features are FP1, FP2, FP3, RXPACC, and DiffP. CIR-PWR was retained because it represents the power amplitude for NLOS propagation characterization [28]. The six main features retained for further selection were FP, Ranging, CIR, First Path Power Level (FPPower), Receive Power Level (RXPower), and Standard Noise Ratio (SNR).

From the six features, the selection was performed using Pearson's correlation. If the secondary dataset is a feature matrix as described in Equations (1), and the primary dataset built (D), where X is the input and y is the target, is described in equation (2), where N is the number of samples and M is the number of initial features. In the equation for the primary dataset $X \in R^{Kx5}$, are five selected features: Ranging, CIR, FPPower, RXPower, SNR. The target y is labeled by $y \in (0,1,2)$ means 0=LOS, 1=NLOS, and 2= multipath.

$$X_{sec} \in \mathbb{R}^{NxM} \tag{1}$$

$$D = \{X, y\} \tag{2}$$

The Pearson correlation to measure the linear relationship (c_{ij}) between features and the target is shown in Equation (3) with $\bar{x}_i = \frac{1}{N}\sum_{k=1}^{N} x_{k,i}$.. The value of N is the number of samples, k is the index of the sample, i is the index of the first feature, j is the index of the target variable, $x_{k,i}$ is the value of feature i for the k_{th} $sample$, and $x_{k,j}$ is the value of feature (or target) for the sample. Features are selected based on the highest correlation to target y, which is the last column in X_{sec} The sorting is descending, and the highest correlation value between features is taken: $F'=\{f'_1, f'_2, \ldots, f'_5\}$ with the correlation value limit and the selected feature are $|c_{ik}, target| \geq \theta$.

$$c_{ij} = \frac{\sum_{k=1}^{N}(x_{k,i} - \bar{x}_i)(x_{k,j} - \bar{x}_j)}{\sqrt{\sum_{k=1}^{N}(x_{k,i} - \bar{x}_i)^2 \sum_{k=1}^{N}(x_{k,j} - \bar{x}_j)^2}} \tag{3}$$

3.2. REGRESSION-ERROR RANGING MITIGATION (REM)

Ranging errors can affect indoor positioning accuracy; therefore, a process is required to minimize distance estimation errors. Therefore, accurate ranging measurements are crucial for building datasets for wireless communication and indoor positioning applications [32]. Error mitigation techniques are essential for minimizing inaccuracies in ranging caused by hardware limitations and environmental interference.

The ESP32 UWB Pro module with a DW1000 chip was used to perform the measurements for dataset development. The module used was the ESP32 UWB Pro with display, which is an integration between the ESP 32 WROOM module. The DW 1000 operates on channels 5 and 6 on the UWB bandwidth. The ESP32 UWB module was selected based on its precision and support for the ToF and TWR techniques.

The ranging accuracy achieved using this module was approximately 10 cm using both ToF and TWR [33]. The use of different UWB modules can provide different performances [34] and can affect the resulting ranging accuracy. The performance of different UWB modules can affect the dataset. Therefore, it is important to understand the ranging error characteristics of the UWB module used so that the error mitigation techniques applied are appropriate.

The REM is a mitigation error method using regression based on a distance estimation error analysis that approximates a normal distribution, which was proposed in previous studies [35]. The ranging error (e_k) is calculated using Equation (4), which is the difference between the actual ranging ($d_{k,\,true}$) and measured ranging ($d_{k,measured}$). The ranging error is analyzed based on the normal distribution parameter $N(\mu_e, \sigma_e^2)$, which is calculated using Equation (5) to obtain a normal distribution curve μ_e with as the mean of the prediction error, σ_e as the sample of standard deviation of the prediction errors, and e_k as the prediction error for the k_{th} sample. The normality of the error analysis results considers regression as a method for mitigating errors.

$$e_k = d_{k,measured} - d_{k,true} \sim \mathcal{N}(\mu_e, \sigma_e^2) \quad for\ k = 1,2, \ldots N \tag{4}$$

$$\mu_e = \frac{1}{N}\sum_{k=1}^{N} e_k \qquad \sigma_e = \sqrt{\frac{1}{N-1}\sum_{k=1}^{N}(e_k - \mu_e)^2} \tag{5}$$

Systematic ranging errors underlies the use of regression using experimental data collected at 1-meter intervals over a 25-meter range. The regression models are created based on Equations (6) where the $d_{corrected}$ is a regression function of distance estimation which denotes the recorded ranging measurement (d_{meas}).

REM was validated by comparing ranging errors before and after mitigation. The validation ensuring that regression significantly improves measurement reliability. The Mean Absolute Error (MAE) in equation (7) is used to evaluate how effective the regression is applied to mitigate ranging errors. $d_{k,\,true}$ is the actual ranging, N is several samples, $d_{k,\,corrected}$ is the mitigation resulting ranging and k is the distance range to 1 m, 2 m, 3 m … and so on.

$$d_{corrected} = f(d_{meas})$$
$$d_{corrected} = \beta_0 + \beta_1 . d_{meas} + \beta_2 . {d_{meas}}^2 \tag{6}$$

$$MAE = \frac{1}{N}\sum_{k=1}^{N}\left|d_{k,true} - d_{k,corrected}\right| \tag{7}$$

3.3. DATASET CONSTRUCTION

The next step was to build the dataset using the PFS-REM method by systematically measuring the five selected features under LOS (Line of Sight), non-line-of-sight (NLOS), and multipath environmental conditions. The five features measured in the measurement are Ranging ($d^{(K_c)}{}_{corrected}$), CIR ($p^{(K_c)}{}_{cir}$), FPPower ($p^{(K_c)}{}_{fp}$), RXPower ($p^{(K_c)}{}_{rx}$, SNR ($s^{(K_c)}{}_{snr}$). Matrix of each condition $c \in$ {LOS,NLOS,MP} is shown in equation (8).

$$\mathbf{X}_c = \begin{bmatrix} d_{corrected}^{(1)} & p_{cir}^{(1)} & p_{fp}^{(1)} & p_{rx}^{(1)} & s_{snr}^{(1)} \\ \vdots & \vdots & \vdots & \vdots & \vdots \\ d_{corrected}^{(K_c)} & p_{cir}^{(K_c)} & p_{fp}^{(K_c)} & p_{rx}^{(K_c)} & s_{snr}^{(K_c)} \end{bmatrix} \tag{8}$$
$$\text{where } \mathbf{y}_c = c \cdot \mathbf{1}_{K_c}$$

The distance feature uses ranging results from regression. Each feature is meticulously measured across the LOS, NLOS, and multipath conditions, ensuring that the dataset captures a comprehensive representation of real-world signal propagation characteristics.

Feature measurements were taken from 1-10 meters, in 1-meter increments. As shown in Fig. 3, the antenna orientations were installed according to realistic positions that could occur in four scenarios., as follows:

- Direct Facing: The anchor and tag antennas face each other.
- Perpendicular Orientation: The tag antennas are oriented 90° to the left and right of the anchor.
- Opposite Facing: The tag antennas are oriented 180° away from the tag.

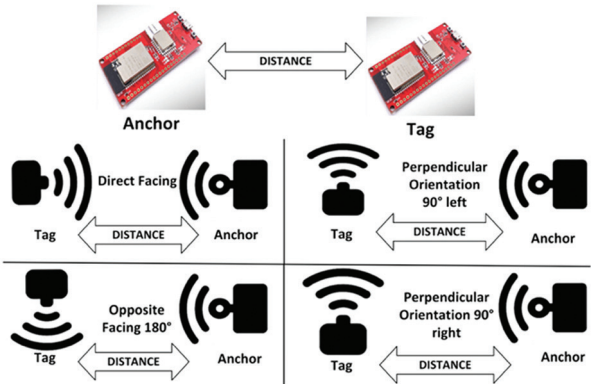

Fig. 3. The antena direction between anchor and tag

These configurations account for practical variations in real-world deployments, where the antenna orientation affects the signal propagation characteristics. Measurements were conducted in three different scenarios: LOS, NLOS, and Multipath environments. Feature dataset measurements in these different environments have the potential to show different ranging performance. Feature measurements in the LOS environment were conducted in an unobstructed room to ensure a clear direct path between the tag and anchor, as shown in Fig. 4(a). In the LOS scenario, ideal conditions occur when signal attenuation and multipath interference are minimal.

(a)

(b)

(c)

Fig 4. Feature measurement scenario: (**a**) LOS, (**b**) NLOS, (**c**) Multipath

Feature measurements for the NLOS dataset were conducted in the same room as the LOS scenario (FIT Hall), with a whiteboard placed as an obstacle between the anchors and tags. This obstacle impedes UWB signal propagation, causing the refraction, diffraction, reflection, and attenuation of the signal. Consequently, the range estimation will have significant deviations. The NLOS scenario is illustrated in Fig. 4(b). The multipath dataset measurements were obtained in a 2.3-meter hallway with walls and wooden doors on both sides, as shown in Fig. 4(c). This environment with adjacent walls causes fading, resulting in constructive and destructive interference. From these measurements, the data will be studied to determine how multipath propagation affects ranging accuracy.

From the measurements, three raw data sets were produced: LOS, NLOS, and multipath raw data. Preprocessing is systematically applied to LOS, NLOS, and Multipath raw datasets (equation 9) before they are integrated into a final dataset that is structured for machine learning classification. Data preprocessing is the process of cleaning data and transforming data into a form that is easier to understand for analysis, including data cleaning, data integration, data transformation, filtering data, renaming columns, dropping duplicate rows, dropping missing or null values, and dropping outliers. The next stage is to combine each LOS, NLOS, and Multipath data to create a dataset that is ready to be used in building a classification model using machine learning.

The next stage involved analyzing each feature in the dataset, including the statistical characteristics of the features, correlations, and evaluations of overfitting and underfitting. The dataset was employed to develop classification models capable of distinguishing between LOS, NLOS, and multipath conditions. The models used were Logistic Regression (LR), Support Vector Machine (SVM), Naïve Bayes (NB), k-nearest neighbors (KNN), Random Forest (RF), Gradient Boosting (GB), and Linear Discriminant Analysis (LDA).

4. RESULT AND DISCUSSION

This section discusses the PFS correlation values, which are subsequently analyzed and used to determine the selected features for dataset construction. In addition, the results of the error analysis were used to derive the regression equation of the REM, which served as the measurement basis for the dataset. Statistical tests and correlation analyses were performed to characterize each feature within the dataset. Underfitting and overfitting tests were conducted to evaluate the reliability of the dataset across different classification models. To obtain a model with high accuracy and low complexity, the classification model results were evaluated based on both accuracy and inference time.

4.1. THE RESULT OF PFS-REM

Fig. 5(a) shows that the Ranging CIR, RXPower, FP-Power, and SNR exhibited strong correlations with each other. This refined feature set was subsequently used to develop the dataset. The modified dataset containing the five selected features was used to build classification models to distinguish between LOS, NLOS, and multipath environments.

The accuracy and complexity parameters were evaluated, as shown in Fig. 5(b). Complexity was measured based on the length of the execution time across all classifiers for both datasets using 12 and 5 features. A comparison of the learning time between datasets using 12 and 5 features showed a significant reduction in the execution time of up to 50% for GB and RF, while still achieving high accuracy. The KNN, LR, and RC models had faster learning times but lower accuracy. The evaluation results show that feature reduction can reduce complexity while maintaining high accuracy in several models, namely, RF and GB.

Error analysis techniques for REM using Q-Q plots and distribution analysis can help identify systematic errors and guide the selection of appropriate mitiga-

tion methods. The systematic ranging errors in this study [35] underlie the use of regression as a mitigation method (REM). Using experimental data collected at 1-meter intervals over a 25-meter range. Fig. 5(c) illustrates the MAE before and after the regression. The effectiveness of the REM-based mitigation was evaluated by comparing the MAE before and after mitigation. The MAE before mitigation was 75.68 cm, and after correction, MAE = 5.05 cm. The post-mitigation results showed a substantial decrease in error across all measured distances, reinforcing the effectiveness of regression as a compensation method. The REM-based error correction significantly reduced the ranging errors, achieving a 93.3% improvement in ranging accuracy. The corrected distance estimates exhibited high reliability, making them suitable for indoor localization and dataset construction.

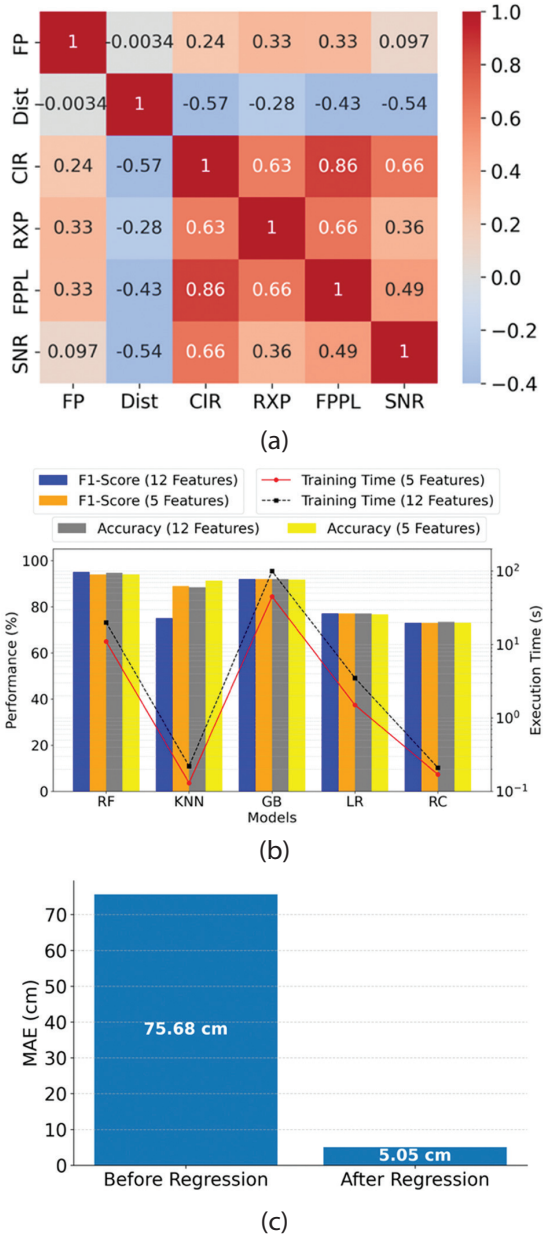

Fig. 5. The result of PFS-REM: (**a**) Pearson correlation heatmap, (**b**) Performance comparison, (**c**) MAE of ranging after and before REM

4. 2. DATASET ANALYSIS

4.2.1. Feature Correlation of The Dataset and Ranging Analysis of each Class

The strongest negative correlation in Fig. 6 (a), with a value of -0.54 for RXPower and Noise, indicates that increased noise interference is associated with a decrease in received power (RXPower). This phenomenon is related to the reflections that occur in NLOS and MP environments. Multipath interference increases noise, thereby reducing the received RXPower. This illustrates that UWB signal propagation is affected by scattering and absorption owing to the presence of reflective and absorptive surfaces.

The correlation between Range and FPPower, with a value of -0.31, indicates that an increase in distance is associated with a decrease in FPPower. In indoor environments, multipath reflections owing to obstacles can cause reflections, accelerating the nonlinear decline in FPPower, particularly under NLOS conditions. In NLOS, the median FPPower value at a range of approximately 1.67 m reached -91.18 dBm, whereas in LOS at a range of approximately 10 m, it reached -79.57 dBm.

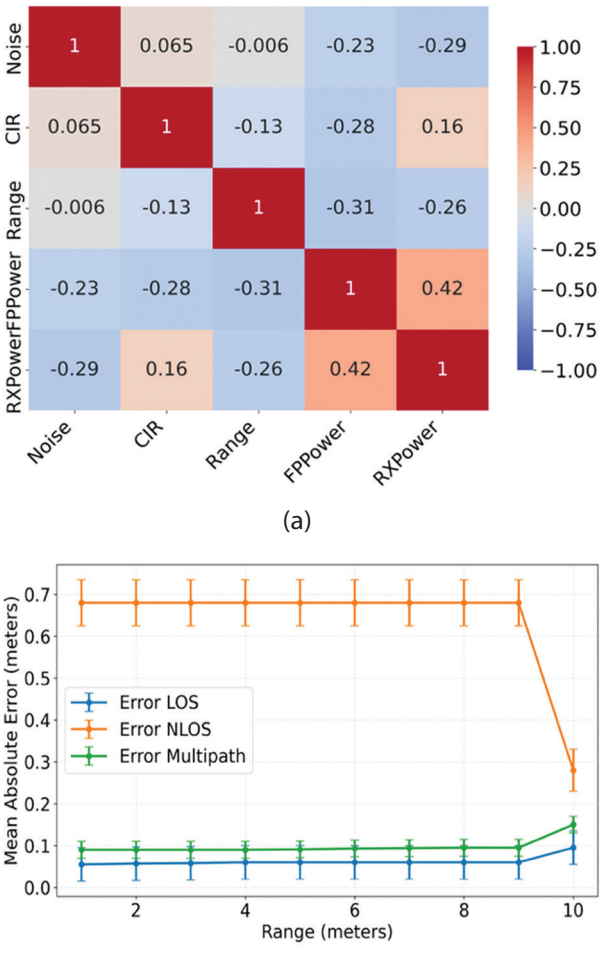

Fig. 6. (**a**) Heatmap Correlation of dataset, (**b**) MAE with standard Deviation of LOS, NLOS, and Multipath

This variability explains the correlation not approaching -1 owing to specific environmental influences, such as absorptive materials that can obscure the distance-power relationship. However, the relationship between RXPower and FPPower was favorable at 0.42. Therefore, as FPPower increases, the overall RXPower increases slightly. RXPower is the total power of the received signal. It is composed of the power from both FPPower and multipath components. The positive correlation of 0.42 indicates that FPPower, which is the main direct signal component, has a substantial effect on RXPower.

This is especially true when LOS is present, because the median FPPower (-79.57 dBm) and RXPower (-57.48 dBm) are more closely related than when NLOS is present (-91.18 dBm vs -58.01 dBm). In other words, FPPower is a simple way to assess signal strength, whereas RXPower is affected by multipath effects, which are stronger in MP situations. Under these conditions, reflections can boost the total received power even if FPPower is lower.

The Ranging (distance) feature is obtained by measuring the distance between the anchor and tag. In the ranging feature, ranging error analysis based on MAE was performed to determine the distance measurement deviations produced by each LOS, NLOS, and Multipath. The standard deviation was calculated to determine the variation in the errors that occurred in LOS, NLOS, and Multipath.

Fig. 6 (b) shows the MAE with error bars for the standard deviation (STD). It shows how well the error works over distances of 1–10 m for three different situations: LOS, NLOS, and Multipath. The MAE numbers show how far off the average range estimate is, and the STD shows how much these readings can change or be incorrect. The MAE for the Multipath condition was moderate and slowly increased from 0.093 to 0.15 m. The standard deviation ranged from 0.025 to 0.027 m. This indicates that the error level was average and the variability was low. This study shows the strength of the LOS ranging, the difficulty of working in NLOS conditions, and the insignificance of multipath effects. This information can help improve range estimation algorithms in different situations.

4.2.2. Feature Statistic Analysis

The SNR boxplot analysis of 16,000 samples in Fig. 7 showed LOS and NLOS with high noise medians of 248 and 276, overlapping ranges of 220-304 and 192-356, and variabilities of 25-30 dBm and 35-40 dBm, respectively, because of identical interference. The MP, which has a median of 124, a limited range of 104 to 144, and low variability of 10 to 15 dBm, shows that interference is managed. Noise is a useful tool for isolating MP because of its clear difference from NLOS, but only a limited distinction between the two.

The line and box graphs of the CIR data show that the complexity is increasing (LOS < MP< NLOS). The line plot (0–16,000 indices) shows NLOS (>30,000, up to 50,000), MP (25,000–35,000), and LOS (<25,000). There is some overlap between the MP and NLOS. The boxplot shows that the medians are 22,183 (LOS), 29,440 (MP), and 30,036 (NLOS), with NLOS exhibiting more variability (>38,000 outliers).

The FPPower boxplot shows that UWB systems have different propagation characteristics compared to others. LOS had the greatest median FPPower at -77.17 dBm, and NLOS had the lowest median at -91.68 dBm. This shows that there is a significant amount of attenuation in the NLOS. MP has a median of -78.78 dBm, a broader range, and more, which demonstrates both direct and reflection effects. The clear distinction (with a small MP-NLOS overlap) shows how well FPPower can differentiate between things, which is why it is used in high-accuracy (>99%) classification models.

The RXPower boxplot analysis shows the differences between the classes. The median for MP was -51.31 dBm, with a range of -56.03 to -50.93 dBm and substantial variability of 2-3 dBm. This is because of the multipath enhancement. The LOS has a consistent median of -57.68 dBm, a small range, and very little variability, which shows direct circumstances. NLOS has the lowest median at -58.00 dBm and minimal variability, which indicates that the signal is blocked. A clear separation between MP and a small overlap between LOS and NLOS shows that RXPower can differentiate between MP, but not as well as FPPower.

4.2.3. Training, Validation, and The Best Model in Accuracy and Complexity

The final stage in producing the dataset was to combine 16,000 LOS raw data samples, 16,000 NLOS raw data samples, and 16,000 multipath raw data samples into one set of 48,000 pre-processed data points. Subsequently, the dataset was split into training and testing sets, with a test size ratio of 0.1 (10%). The analysis based on accuracy and complexity is shown in the performance graph in Fig. 8 and the learning curve in Fig. 9.

LR and LDA, on the other hand, have median accuracies that are lower, between 0.84 and 0.85. They may also have lower-end outliers, which means that linear models cannot fully capture the nonlinear complexity of features such as FPPower and CIR in the UWB dataset. LR and LDA learning curves demonstrate underfitting characteristics, evidenced by consistently low validation scores and minimal gaps. This indicates the constraints of linearity and Gaussian assumptions in capturing complex nonlinear feature interactions, particularly the significant correlation between Range and FPPower.

Naïve Bayes exhibits underfitting because of breaches in the feature independence assumption. The median accuracy of NB is between 0.85 and 0.86, which means that the data are slightly more spread out. SVM, on the other hand, is approximately 0.95% accurate on average, which means that it can be used in many different scenarios.

Fig. 8 illustrates the performance of the LR, SVM, NB, KNN, RF, GB, and LDA classification models on the LOS, NLOS, and Multipath datasets after five rounds of cross-validation (5-fold CV). RF and GB are near the top, with median accuracies close to or higher than 0.99. The boxes are not very wide; therefore, there is not much variance, and there are no large outliers.

This implies that the predictions regarding the spread of signals are quite accurate.

KNN also performed well, with median accuracies of approximately 0.98–0.99. There may be some outliers on the lower end, however, because it is sensitive to how far apart neighbors are in data distributions that are not even.

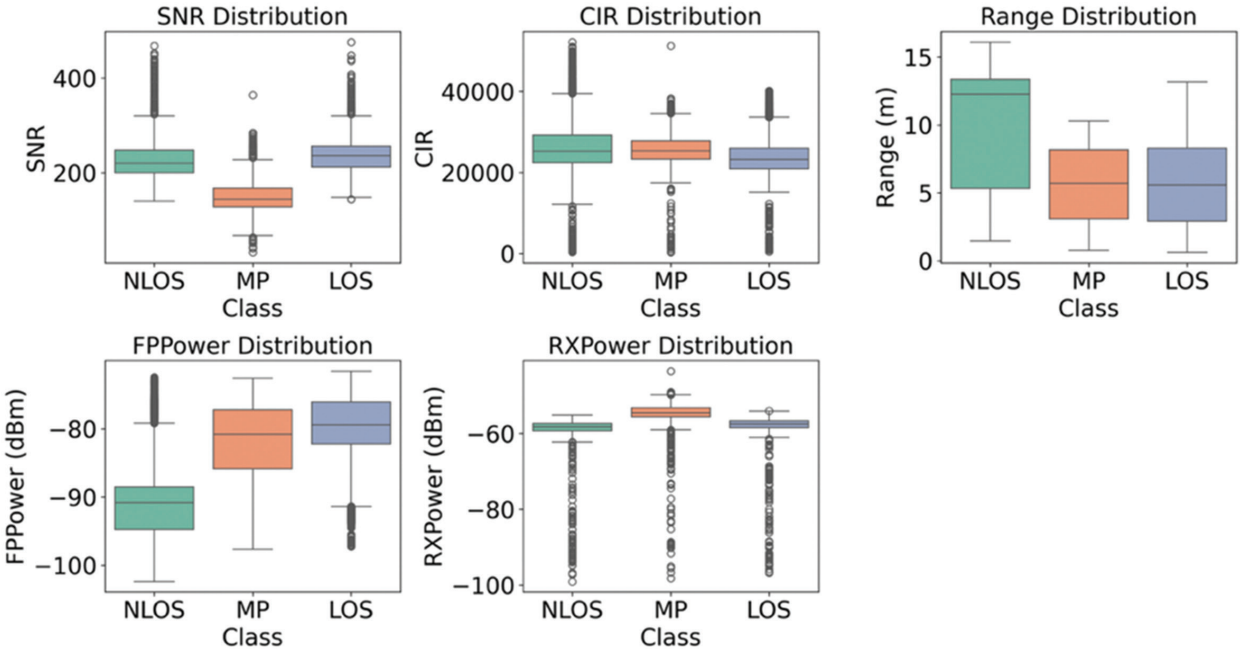

Fig. 7. Boxplot Diagram of each feature distribution

Fig. 8. Learning curve of each model

The learning curves in Fig. 9 illustrate the model behavior patterns that indicate the trade-off between bias and variance, along with the generalization capability across datasets characterized by LOS, NLOS, and MP class distributions. KNN indicates a slight local overfitting that is manageable, whereas RF and Gradient Boosting consistently deliver superior performance by utilizing aggregation and boosting techniques that effectively minimize variance and residual bias. These patterns indicate that nonlinear ensemble methods are the most dependable for classifying complex UWB signal propagation conditions.

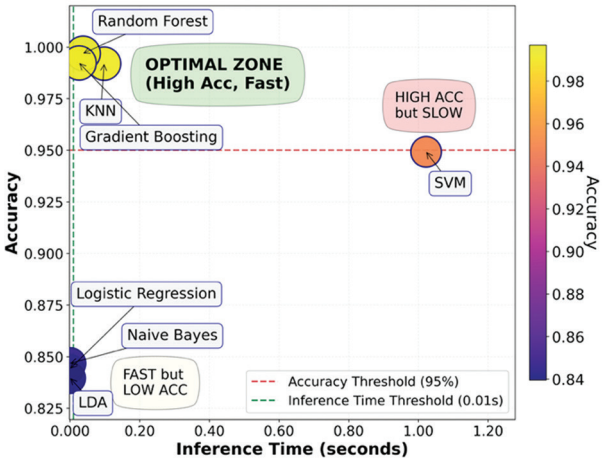

Fig 9. Model Performance accuracy vs Inference Time

In contrast, nonlinear models such as KNN, RF, and GB demonstrated significantly enhanced generalization performance, with validation scores nearing 0.98–0.99 and minimal discrepancies, along with low standard deviations (<0.02) that reflect stable performance estimates. KNN indicates a slight local overfitting that is manageable, whereas RF and Gradient Boosting consistently deliver superior performance by utilizing aggregation and boosting techniques that effectively minimize variance and residual bias. These patterns indicate that non-linear ensemble methods are the most dependable options for classifying complex UWB signal propagation conditions.

The statistically significant differences in the median values between the models, especially between the linear and ensemble-based models, show that RF and GB are the best choices for UWB categorization. However, linear models may not perform well. This can be resolved by either using nonlinear methods or providing more information.

Inference time is a real-world method for measuring the complexity of a model [36, 37]. Inference time is the time required for a trained machine learning model to predict new input data. Models with more complex structures or computations, such as deep or ensemble architectures, usually require more time to make predictions because they have more parameters, layers, or operations. Simpler models, like linear classifiers, on the other hand, often make inferences faster but don't represent as much information. By comparing the accuracy and inference time of each model, we can determine which model is optimal in terms of complexity and accuracy. Models with low complexity and high accuracy are particularly useful when applied to resource-constrained environments or real-time positioning, where latency is critical. Inference time measurements reflect not only the computational cost but also the scalability, applicability, and responsiveness of each model.

LR, SVM, NB, KNN, Random Forest, Gradient Boosting, and LDA were used on the UWB dataset to figure out what kind of propagation conditions there were: LOS, NLOS, or multipath. Fig. 7(b) shows the balance between the accuracy of the model and the time required to make an inference. RF is an excellent example of how ensemble bagging can help models perform better on new data. It is approximately 0.997% accurate and takes approximately 0.003 seconds to make a guess. It also works well to lower the variance in features such as FPPower and RXPower, which have strong negative correlations (r = -0.98 with Range).

KNN has very strong non-parametric decision boundaries, with an accuracy of 0.994 and a time of 0.045 s. However, it takes longer to determine things because it must determine distances in a space with many dimensions. GB ranked second with an accuracy of 0.991 and an inference time of 0.002 s. Sequential boosting reduces bias in situations with more than one path.

SVM achieved a high accuracy of 0.95, but the resulting inference time was quite long compared with those of GB and RF. Meanwhile, models with low accuracy, such as LR, NB, and LDA, showed underfitting; therefore, these models are not recommended. Linear-based models produce less accurate discrimination between LOS, NLOS, and Multipath classes because they do not consider the nonlinearities in the characteristics of the UWB signal dataset.

Therefore, a trade-off occurs in datasets with correlated features, such as SNR and RX Power, so a fast inference time leads to high deviations.

5. CONCLUSION

The development of the PFS–REM dataset provides a compact and representative data foundation for identifying LOS, NLOS, and multipath signal propagation conditions in ultra-wideband (UWB)-based localization systems. The PFS–REM method applied to the dataset effectively reduced feature dimensionality while significantly maintaining the classification model accuracy. The results of the feature characterization analysis revealed consistent differences in the propagation patterns across the LOS, NLOS, and multipath classes. This demonstrates the strong discriminatory capabilities of the dataset, resulting in accurate models.

The optimal models with low complexity but high accuracy are RF and GB, which achieve an accuracy exceeding 99%. The findings of this study confirm that the PFS–REM-based approach is a practical solution for reducing complexity while maintaining high accuracy and efficiency in UWB indoor positioning, particularly when implemented for real-time applications and resource-constrained devices.

Further research should focus on developing a dataset that addresses obstacle material types, multipath corridor widths, and antenna direction. Furthermore, exploration of each feature, such as feature extraction, could be conducted to identify patterns that can generalize the dataset to indoor conditions. The proposed model implementation in this study could be applied to edge computing, and its performance could be observed in positioning and tracking applications in the future.

REFERENCES

[1] X. You, D. Tian, C. Liu, X. Yu, L. Song, "Vehicles positioning in tunnel: A real-time localization system using DL-TDOA technology", Journal of Internet Technology, Vol. 22, No. 5, 2021, pp. 967-978.

[2] K. Mascher, M. Watzko, A. Koppert, J. Eder, P. Hofer, M. Wieser, "NIKE BLUETRACK: Blue Force Tracking in GNSS-Denied Environments Based on the Fusion of UWB, IMUs and 3D Models", Sensors, Vol. 22, No. 8, 2022.

[3] W. Shule, C. M. Almansa, J. P. Queralta, Z. Zou, T. Westerlund, "UWB-Based Localization for Multi-UAV Systems and Collaborative Heterogeneous Multi-Robot Systems", Procedia Computer Science, Vol. 175, 2020, pp. 357-364.

[4] C. Lian, S. Referent, I. Ulrich, R. Korreferent, I. U. Witkowski, "Bidirectional UWB Localization with Rigorous Sectoral Evaluations", arXiv:2302.07706v2, 2023.

[5] Itu-r, "Impact of devices using ultra-wideband technology on systems operating within radiocommunication services SM Series Spectrum management", http://www.itu.int/ITU-R/go/patents/en (accessed: 2025)

[6] N. El-Sheimy, Y. Li, "Indoor navigation: state of the art and future trends", Satellite Navigation, Vol. 2, 2021, p. 7.

[7] J. Kunhoth, A. G. Karkar, S. Al-Maadeed, A. Al-Ali, "Indoor positioning and wayfinding systems: a survey", Human-centric Computing and Information Sciences, Vol. 10, 2020, p. 18.

[8] G. I. Hapsari, R. Munadi, B. Erfianto, I. D. Irawati, "Future Research and Trends in Ultra-Wideband Indoor Tag Localization", IEEE Access, Vol. 13, 2024, pp. 21827-21852.

[9] G. I. Hapsari, R. Munadi, B. Erfianto, I. D. Irawati, "Research Trend Topic Area on Mobile Anchor Localization: A Systematic Mapping Study", International journal of electrical and computer engineering systems, Vol. 14, No. 9, 2023, pp. 959-972.

[10] J. Ninnemann, P. Schwarzbach, O. Michler, "Toward UWB Impulse Radio Sensing: Fundamentals, Potentials, and Challenges", UWB Technology - New Insights and Developments, IntechOpen, 2023.

[11] F. Che, Q. Z. Ahmed, F. A. Khan, P. I. Lazaridis, "Feature-Based Generalized GaussianDistribution Method for NLoS Detectionin Ultra-Wideband (UWB) IndoorPositioning System", IEEE Sensor Journal, Vol. 22, No. 19, 2022, pp. 18726-18739.

[12] F. Che, W. Bin Abbas, Q. Z. Ahmed, B. Amjad, F. A. Khan, P. I. Lazaridis, "Weighted Naive Bayes Approach for Imbalanced Indoor Positioning System Using UWB", Proceedings of the IEEE International Black Sea Conference on Communications and Networking, Sofia, Bulgaria, 6-9 June 2022, pp. 72-76.

[13] H. Yang, Y. Wang, C. K. Seow, M. Sun, M. Si, L. Huang, "UWB Sensor-Based Indoor LOS/NLOS Localization With Support Vector Machine Learning", IEEE Sensor Journal, Vol. 23, No. 3, 2023, pp. 2988-3004.

[14] A. S. Syathirah, R. Munadi, G. I. Hapsari, "Enhancement of Accuracy For UWB Indoor Positioning Using Support Vector Regression", Proceedings of the IEEE International Conference on Communication, Networks and Satellite, Mataram, Indonesia, 28-30 November 2024.

[15] Z. Gao, Y. Jiao, W. Yang, X. Li, Y. Wang, "A Method for UWB Localization Based on CNN-SVM and Hybrid Locating Algorithm", Information, Vol. 14, No. 1, 2023.

[16] M. Si, Y. Wang, H. Siljak, C. K. Seow, H. Yang, "A lightweight CIR-based CNN with MLP for NLOS/LOS

identification in a UWB positioning system", IEEE Communications Letters, Vol. 27, No. 5, 2023, pp. 1332 - 1336.

[17] C. L. Sang, B. Steinhagen, J. D. Homburg, M. Adams, M. Hesse, U. Rückert, "Identification of NLOS and multi-path conditions in UWB localization using machine learning methods", Applied Sciences, Vol. 10, No. 11, 2020.

[18] L. Flueratoru, E. S. Lohan, D. Niculescu, "Self-Learning Detection and Mitigation of Non-Line-of-Sight Measurements in Ultra-Wideband Localization", Proceedings of the International Conference on Indoor Positioning and Indoor Navigation, Lloret de Mar, Spain, 29 November - 2 December 2021.

[19] W. Zhao, A. Goudar, X. Qiao, A. P. Schoellig, "UTIL: An ultra-wideband time-difference-of-arrival indoor localization dataset", International Journal of Robotics Research, Vol. 43, No. 10, 2024.

[20] Z. Cui, T. Liu, S. Tian, R. Xu, J. Cheng, "Non-Line-of-Sight Identification for UWB Positioning Using Capsule Networks", IEEE Communications Letters, Vol. 24, No. 10, 2020, pp. 2187-2190.

[21] C. L. Sang, M. Adams, T. Hörmann, M. Hesse, M. Porrmann, U. Rückert, "Numerical and Experimental Evaluation of Error Estimation for Two-Way Ranging Methods", Sensors, Vol. 19, No. 3, 2019, pp. 24-27.

[22] A. F. Majeed, R. Arsat, M. A. Baharudin, N. M. Abdul Latiff, A. Albaidhani, "XGBoost Based Multiclass NLOS Channels Identification in UWB Indoor Positioning System", Computer Systems Science and Engineering, Vol. 49, No. 1, pp. 159-183, 2025.

[23] V. Barral, C. J. Escudero, J. A. García-Naya, R. Maneiro-Catoira, "NLOS identification and mitigation using low-cost UWB devices", Sensors, Vol. 19, No. 16, 2019.

[24] M. Liu, X. Lou, X. Jin, R. Jiang, K. Ye, S. Wang, "NLOS Identification for Localization Based on the Application of UWB", Wireless Personal Communications, Vol. 119, No. 4, 2021, pp. 3651-3670.

[25] Q. Wang et al. "1D-CLANet: A Novel Network for NLoS Classification in UWB Indoor Positioning System", Applied Sciences, Vol. 14, No. 17, 2024.

[26] S. Wang, N. S. Ahmad, "Robust Classification of UWB NLOS/LOS Using Combined FCE and XGBoost Algorithms", IEEE Access, Vol. 12, 2024, pp. 151030-151045.

[27] S. Wang, N. S. Ahmad, "Improved UWB-based indoor positioning system via NLOS classification and error mitigation", Engineering Science and Technology, an International Journal, Vol. 63, 2025.

[28] J. Resti, G. I. Hapsari, R. Munadi, B. Erfianto, I. D. Irawati, "Feature Selection Using Pearson Correlation for Ultra-Wideband Ranging Classification", Jurnal RESTI (Rekayasa Sistem dan Teknologi Informasi), Vol. 10, No. 2, pp. 209-217, 2025.

[29] S. Kram, M. Stahlke, T. Feigl, J. Seitz, J. Thielecke, "UWB channel impulse responses for positioning in complex environments: A detailed feature analysis", Sensors, Vol. 19, No. 24, 2019.

[30] C. Guo, "KNCFS: Feature selection for high-dimensional datasets based on improved random multi-subspace learning", PLoS One, Vol. 19, No. 2, 2024.

[31] C. L. Sang, "Identification of NLOS and MP in UWB using ML (Dataset)", https://github.com/clian-sang/Identification-of-NLOS-and-MP-in-UWB-using-ML (accessed: 2025)

[32] J. Sidorenko, V. Schatz, N. Scherer-Negenborn, M. Arens, U. Hugentobler, "Error Corrections for Ultrawideband Ranging", IEEE Transactions on Instrumentation and Measurement, Vol. 69, No. 11, 2020, pp. 9037-9047.

[33] "ESP32-WROVER Datasheet", www.espressif.com/en/subscribe (accessed: 2025)

[34] B. Morawska, P. Lipinski, K. Lichy, P. Koch, M. Leplawy, "Static and Dynamic Comparison of Pozyx and DecaWave UWB Indoor Localization Systems with Possible Improvements ", Proceedings of Computational Science - ICCS 2021: 21st International Conference, Krakow, Poland, June 16-18 2021.

[35] G. I. Hapsari, R. Munadi, B. Erfianto, I. D. Irawati, "Accuracy Improvement for Indoor Positioning Using Decawave on ESP32 UWB Pro with Display and Regression", Journal of Robotics and Control, Vol. 5, No. 3, 2024, pp. 851-862.

[36] R. Manvi, A. Singh, S. Ermon, "Adaptive Inference-Time Compute: LLMs Can Predict if They Can Do Better, Even Mid-Generation", arXiv:2410.02725, 2024.

[37] D. Trihinas, P. Michael, M. Symeonides, "Evaluating DL Model Scaling Trade-Offs During Inference via an Empirical Benchmark Analysis", Future Internet, Vol. 16, No. 12, 2024.